PETROLEUM SOCIETY
CANADIAN INSTITUTE OF MINING, METALLURGY & PETROLEUM

PAPER 2004-104

CANADIAN INTERNATIONAL PETROLEUM CONFERENCE

Small-Diameter Gas Lift Systems—A Viable Technical Solution for Transport of Fluids From Low-Pressure Reservoirs

J.A. BECARIA
University of Alberta

P. TOMA
P. R. Toma Consulting Ltd

E. KURU
University of Alberta

This paper is to be presented at the Petroleum Society's 5th Canadian International Petroleum Conference (55th Annual Technical Meeting), Calgary, Alberta, Canada, June 8 – 10, 2004. Discussion of this paper is invited and may be presented at the meeting if filed in writing with the technical program chairman prior to the conclusion of the meeting. This paper and any discussion filed will be considered for publication in Petroleum Society journals.

Abstract

Production of fluids from low-pressure reservoirs requires a continuous or an intermittent artificial lifting technology. If the shut-in fluid level is less than 20% of the depth of the well finding a suitable and economic artificial lifting technology is a challenging task. Depending on local conditions and economics,

gas or steam lifting alone or associated with other artificial lifting technologies is selected.

Within a limited range of gas-liquid flowrates, use of small-diameter gas lifting technology is better suited than the gas lifting using conventional tubing to produce liquids from low-pressure reservoirs.

Laboratory investigations dedicated to small-diameter gas lifting operations have been so far limited to fluid transfer operations requiring maximum 10-20 m. This study responds to the industry need for a better evaluation of depth – diameter flowrates limitations in view of assessing the potential field application of gas lifting for very low reservoir pressures and relatively small liquid flowrates.

Production of oil and gas from pressure-depleted reservoirs, recovery of methane from coalbed reserves, and efficient drainage of heavy oil and saturated high-temperature condensate produced under steam-assisted gravity methods, where reservoir pressure is marginally low, require a re-visiting of conventional artificial lifting technologies.

For example, there are thousands of dormant gas wells where bottom water aquifers of 50 m or less impede gas production. Similar conditions are often found in the coalbed methane reservoirs. Use of submersible electric pumps for low-pressure, low liquid production reservoirs is rarely an economic or a viable technical option.

The availability of gas and the relatively small amount of liquid to be transferred suggest gas lifting as a potential strategy for producing the reservoir water and releasing the gas. However, conventional gas lifting (using tubes with a diameter D>1 in.) is not possible due to the extreme low

reservoir pressure conditions. Small diameter pipes (D<1 in.) were occasionally used for gas lifting operations in such fields with mixed results.

In this paper, a critical review of the existing literature on the numerical evaluation methods of gas lifting was presented first. Laboratory tests were conducted by using a specially designed rig and the results were used to evaluate the accuracy of the existing model predictions. Experimental results were also used for assessing the effect of gas-liquid flowrate and interfacial tension on the liquid production rate and flowing bottomhole pressure.

Experimental data were further used for developing a model to determine critical limit of the small diameter gas lifting technique under field conditions. The new model, better adapted for the needs of the industry, can be used to transfer laboratory information to the field scale.

Introduction

Gaslifting or airlift has been used to remove water from flooded mines since 1782[1-2]. Today, natural gaslifting is commonly used for oil wells where gas and liquid are produced together.

Conventional gaslifting uses tubing (or ducts) with a diameter greater than 1 in. Vertical upward transport of gas and liquid for such conditions is well investigated and both empirical[3] and mechanistic models are available.[4-6] Flow pattern mapping and drift-flux model[7] for evaluating the gas-liquid relative velocities are currently used to accurately calculate production-pressure conditions for natural and artificial gas lifting operations. During the last twenty years, mechanistic models replaced most of the empirical models.

Development of a mechanistic approach uses: a. extensive visual observations on field-scaled laboratory models, b. assessment of the main gas-liquid features (type of bubbles, liquid film, etc.) and of the phases interface aspect, c. estimation of local gas and liquid velocities including the slip, d. estimations of local void fraction and of static and dynamic pressures, e. computer-assisted integration of "local" features to include the pressure-volume-temperature modifications for large pressure/ temperature variations (for deep/long pipes or wells), f. field validation.

However, gas-liquid flow in small-diameter tubes to replace conventional gas lifting for special field production strategy is still an un-mapped territory.

Within an optimal operation range of gas-liquid flowrates, small-diameter gas lift is better suited to produce from low-pressure reservoirs as compared to conventional gas lift.

When optimal limits are exceeded, frictional pressure drop (generally less important than static pressures) become important and the advantage offered by small-diameters with gas-liquid flow is lost.

The following section is a summary of the tubing diameter effect on the liquid production rate in gas lifted wells.

From Conventional To Small-Diameter Gas Lifting

Conventional gas lifting (with tubing diameter of 1 in and larger) has been extensively used in the past [2] to decrease the effect of static pressure in vertical wells and increase liquid production. More recently gas lifting was extended to produce stripper wells and enhance waterflood operations[8].

For a certain inflow performance relationship (IPR) (i.e., expressing the well production Q_L as a function of bottom hole pressure – BHP) - the production potential is established by cross-plotting the IPR curve with the BHP-flowrate characteristic of the well.

For situations where compressed gas is injected from surface, the point of gas injection and the gas injection rate are essential to determine and optimize the production rate. The numerical solution is obtained by simply balancing the flowing BHP with the sum of the static and frictional pressure drops calculated for a certain tube diameter D, and for a certain gas and liquid flowrate Q_L, Q_G (eq. 1).

The total depth of the well is divided into n joints, for each joint the entrance pressure and temperature $(P,T)_{in}$ are considered constant, the calculated exit $(P,T)_{ex}$ are used as entrance values for the next joint.

$$P_{res} = \sum_{1=1}^{n} \left(\Delta P_{fr} + \Delta P_{st}\right)_{D,Q_G,Q_L} \qquad (1)$$

Accurate estimation of static pressure drop, usually much larger than frictional one, requires a good knowledge of actual gas-liquid velocities, essential to estimate the local phase allocation and density. Actual gas/liquid velocities depend on total transport velocity and on the phase slip velocity.

Equation 2a is a simplified version of drift-flux model and expresses the value of local gas velocity U_G as a function of transport velocity U_m (eq.2b) and terminal (rising) velocity, u_t. The terminal (rising) velocity depends on the type of gas bubble and flow pattern determined before for local flow conditions.

$$U_G = cU_m + u_t \qquad (2\text{-a})$$

$$U_m = U_G^S + U_L^S = \frac{Q_G + Q_L}{A} \qquad (2\text{-b})$$

The slug flow, illustrated in figure 1, is one of the most common flow pattern encountered in conventional gas lifting systems. Bubble-flow and annular flow patterns are also observed, though, at much lower gas velocities and at extreme high gas velocities, respectively. The bubble flow is discussed as a sub-pattern of conventional slug flow. Annular flow is not analyzed in this paper.

A (conventional) slug flow pattern (fig. 1) is composed of a Taylor-Dumitrescu[9] (TD) "bullet-shape" bubble with a diameter close to the pipe diameter (a thin liquid film separates the bubble from the tube) followed by a swarm of gas bubbles. The typical bubble populating the swarm in the turbulent tailing edge of the TD bubble (named "Harmathy" – "H") has an ascending velocity almost independent of its size,[11] (a common equivalent spherical diameter is d_H=6-12 mm). The two-(sub) pattern slug formation repeats itself in a statistical identical manner as long as the fluid properties are unchanged.

Accurate estimation of the length of each sub-system (see numerical modeling) and of terminal/ascending velocities of TD bubble and bubble swarm are essential to any calculation of gas-liquid allocation (void fraction).

The major differences in characteristics of gas-liquid flow observed in conventional and small diameter gas lifting process can be summarized as follows:

1. As the diameter of the tube is reduced to sizes comparable to the equivalent diameter of "H" bubble, the typical slug pattern is first distorted, then disappear. For tubes smaller than approximately D=20 mm the "H" bubble cannot exist anymore. The wobbling, non-spherical features of "H" bubble are conditioned by a pipe diameter ($D>>d_H$) and this condition is not fulfilled with small-diameter gas lifting. Therefore, all existing models and calculations taking this sub-pattern into considerations are not valid for small-diameter pipes (this observations applies to "conventional" calculation models used to assess the experiments in this paper).
2. Conventional calculations are assuming that the (fall-back) liquid film interposing the ascending TD bubble and the vertical pipe has a negligible thickness as compared to the pipe diameter or to the TD bubble diameter. In some models[5], the effect of the fall-back film is considered negligible when compared to the total amount of liquid found in a slug gas-liquid system. This assumption has to be re-visited for small-diameter pipes. In small-diameter pipes, falling of the film is controlled by the interfacial tension effect and by the fact that a planar, "flat-film" assumption is no longer valid.
3. For conventional gas lifting calculations, as a result of #2, the effect of interfacial tension is generally omitted. It appears only indirectly when the terminal ascending velocity of "H" bubble is considered (condition invalidated by "small-diameter").
4. A relatively high-turbulent regime is associated with conventional slug-flow pattern. The turbulent-dissipated energy[10] is responsible for formation of "H" bubbles by breaking of the tailing-edge of TD bubble (a dynamic breaking-coalescence process maintains the size and bubble composition almost constant). For small-diameter tubes, the turbulent flow condition is invalidated; first by the diameter, then by the low liquid transport velocities.
5. The terminal (upward) velocity $u_{t(T-D)}$ of a T-D bubble depends in great extent on the tube diameter D (Equation 3). Therefore it is expected that with decreasing of tube diameter, the local gas allocation to increase with beneficial effects (reduction local gas-liquid density and of static pressure component). However, the rising of gas bubble in small-diameter pipe is not identical and requires further investigations.

$$u_{t(T-D)} = k\sqrt{gD} \qquad (3)$$

No need was indicated in the past for the use of small-diameter tubing artificial lifting strategy to produce wells at relatively small liquid rates. However, currently, such a need exists in the industry, particularly, to unload water from wells producing gas from coalbed methane reservoirs or from depleted gas reservoirs.

In order to evaluate similarities and differences between gas-liquid transportation in conventional and small-diameter tubes, conventional models are used first to produce base-line information and evaluate the effect of reducing the diameter of the tubing on production characteristics.

The Effect of Tube Diameter

Minimum required reservoir pressure (for fixed production conditions) is calculated as function of tube diameters.

Ansari [5] and Hasan[6] models for conventional tubes where used to investigate the effect of tubing diameter on the liquid production rate and to determine the minimum reservoir pressure required for the onset of the liquid production.

Figure 2 illustrates a "U" shape curve describing the effect of tube diameter on the minimum reservoir pressure required for producing a fixed amount of liquid. For tubing diameters greater than $^3/_4$ in the two models compares satisfactorily, however, for $^1/_2$ in tubing the two models are producing essential different results. Figure 2 also indicates that with $^3/_4$ in diameter tubing water can be produced from 200 m depth when a minimum 50 m of static water column (reservoir pressure equivalent) is available. (BHP=500 KPa, S=25%).
Figure 2 suggests that an optimum range of pipe diameters should be exploited for producing fluids from reservoirs with very low BHP. However, the use of small-diameter pipes in field applications is not common. A large number of laboratory investigations and industrial applications using small diameter gas (air) lift over a few meters of elevation were reported[11-13], but no attempts have been made to assess physical limitations resulting from a considerable increase of the tube length (i.e., a few hundred meters of vertical transport) to accommodate field application.

For one-injector gas operations in the field using tubes of 1 to 5 in diameter a minimum submergence S=50% is required (i.e., for a depth of 1000 m, the reservoir pressure should be sufficient to maintain a shut-in fluid level of approximately 500 m).

Preliminary calculations (using conventional models) suggest that reducing the tube diameter is a viable alternative and improving the numerical estimation is required.

Laboratory rig

To investigate the effect of small-diameter on production performances and further aid to development and validation of a suitable numerical model for transferring laboratory results to field depth conditions, a laboratory experimental rig was built and used.
Figure 3 is a schematic of field and laboratory gas lifting.

The laboratory experiments where operated to simulate extreme field conditions in depleted reservoirs with very low pressure e.g. h/L ratios < 0.2 were used.

Water and water-methanol mixtures were used. For each specific concentration and room temperature the interfacial tension was separately measured.
A certain experimental run is defined by: a. tube D (mm) b. injected gas flowrate Q_G (liter/min), c. simulated reservoir pressure P_{res} (simply expressed by the level "h"),
d. Water-methanol composition and interfacial tension.

For each run the measured values include:
a. Produced liquid rate, Q_L (liter/min), b. average injection pressure, P_{in} (equivalent to BHP) c. Maximum and minimum momentary pressures recorded over 5 min (reflecting pressure oscillations and specific instability conditions).

For a certain tube diameter and reservoir pressure, a production characteristic was obtained by performing a step increase of the injected gas. At each level of injection (maintained constant for approximately 20 min), the production of liquid (returned to the reservoir) was measured. During each step, the gas flowrate was measured (using a rotameter and a digital flowmeter) and

injection pressure was separately recorded using an average and a momentary metering systems.

In addition, visual and photographic evidence of the observed main gas-liquid features specific to each series of experiments were recorded. A summary of the experimental results leading to a laboratory-field transfer model is further discussed.

Reservoir Pressure and Submergence

The reservoir pressure is given by (notations in fig. 3):

$$P_{res}=\rho g h \qquad (4)$$

Where ρ is the average density of liquid (water and methanol mixture for laboratory)

The ratio between the distance from injector to the liquid level to the distance from injector to the wellhead (equation 5), named submergence (S), is commonly used for rapid assessment of a gaslifting system.

$$S = \frac{h}{L} 100\ (\%) \qquad (5)$$

The laboratory design (fig. 3b) includes all the key elements of a field gaslift. The tube diameter is not scaled. The length of the vertical tube section (L_{lab}) is approximately 3 m.

Laboratory Results

The results of laboratory investigations regarding the effects of reservoir pressure, tubing diameter and interfacial tension on the liquid production rate with small diameter tubes are presented.

Reservoir Pressure and Tubing Diameter

Figure 4 illustrates the effect of gas injection on the liquid production rate for D=12 mm and h=63.5 and 38 cm (simulated reservoir pressures).

Three production-related features are noticed in fig. 4:
a. The onset of liquid production: For h=38cm the production is initiated for gas injected in excess of 4 l/min; for 63.5 cm only 2 l/min of gas injected is required. The reservoir pressure and gas injection rate required to initiate the production are identified as "critical production conditions".

b. The effect of (reservoir) pressure: Increasing the pressure has a significant effect on production; e.g. at the same gas injection of 6 l/min (fig. 4) for a 65% increasing the reservoir pressure (from h=38 to 63 cm) enhanced the liquid production approximately six times (from 0.1 l/min to 6 l/min).

c. The submergence: The relative reservoir pressure or submergence (S eq.5) required for an active fluid production is considerably smaller in the laboratory (S=12.7% for h=38 cm) than the value required in the conventional field operations.
This is not only related to the positive effect of small-diameter tubing, but in some extent, to the effect of the absolute depth used in laboratory experiments (L=3m). The net effect of liquid production is a compounded result of upward transport of gas-liquid and of the liquid film fallback. It is expected that the negative fallback film flow will increase with increasing the well depth.

Tube Diameter

Laboratory observations on the effect of tube diameter on production offer valuable information regarding process optimization and limitations. However, laboratory information cannot be directly extrapolated to field conditions. In order to better evaluate the small diameter pipe effect for field conditions, laboratory results were first validated using a simplified numerical model. The model was further used for assessing the potential use of small-diameter tubing for field conditions.
Figure 5 illustrates the production characteristics (liquid produced versus gas injected) with 4, 7.8 and 12 mm tubings, all operated at the same simulated reservoir pressure of 63.5 cm. For a range of gas injection rates between 2 and 3.5 liter/min ("A"), the liquid production rate obtained with 7.8 mm tube exceeds the 12 mm. For smaller or larger injection rates, the situation is different; at higher injection rates, 12 mm tubing indicates a higher production rate.

Figure 6 is a detail of figure 5 for low gas injection conditions. For gas injection rate below 0.5 l/min, the 4 mm tube performs better than 7.8 mm tube. Between 0.5 to 1 l/minutes 4 and 7.8 mm tubes performances are comparable.

$$U_G^S = \frac{Q_G}{A} \quad (m/s) \qquad (6\text{-a})$$

$$U_L^S = \frac{Q_L}{A} \quad (m/s) \qquad (6\text{-b})$$

Use of superficial velocities (eqs. 6a,b and fig. 7) offers a better way to compare production characteristics for different operating conditions. Within a superficial gas velocity of 1.5 and 2.2 m/s a maximum (specific) production rate is observed for all three investigated tube diameters.
For maximum liquid ranges, figure 7 also shows that the 7.8 mm tube yields higher specific liquid production rates than 4 and 12 mm diameter tubes.

Regardless of whether the actual flowrates or superficial velocities are selected to display the tube production characteristic, a maximum productivity situation is observed and exploited. This is a zone where the derivative of liquid production (or superficial liquid velocity) with respect to the sum of frictional and static pressure drops (eq. 1) approaches zero (equation 7). The sign of the second derivative has to be analyzed for achieving the maximum conditions.

$$F_{opt.prod} = \left[\frac{\partial(Q_L)}{\partial\left(\frac{\Delta P_{st} + \Delta P_{fr}}{\Delta L} \right)_{Q_G, Q_L}} \right]_{\text{from 0 to} L} = 0 \qquad (7)$$

The Effect of Interfacial Tension

Using a mixture of water and methanol in different proportions offers the possibility to observe the effect of interfacial tension in a range of approximately 35 to 70 dynes/cm. Changing the

interfacial tension has a direct effect on the rate of fallback film and offers a simple method to assess this aspect specific to small diameter tubes.

Figure 8, using superficial liquid velocity versus superficial gas velocity, compares production characteristics obtained with D=12 mm h=63.5 cm (water only, σ= 72 dyne/cm) and water-methanol (σ = 38 dyne/cm). Reduction of interfacial tension from 72.4 to 38 dyne/cm has a negative impact on the liquid produced. At U_{gs}= 1.5 m/s the superficial liquid velocity (specific production rate) obtained for methanol-water is 23% lower than the superficial liquid velocity measured for water only (a decrease from 0.105 to 0,08 m/s).

Experiments using D=7.8 mm (conducted under the same conditions as the ones using 12mm shown in figure 8) indicated a 33% decrease in liquid production rate when water is replaced by water-methanol mixture.

The effect of interfacial tension on gas lifting performances will be further used to validate an "in-house" numerical model designed for gas lifting with small-diameter tubing.

Qualitative (visual) Observations

Pseudo-slug gas bubbles were generally observed during the flow of air-water and air-water-methanol fluids through 12 mm tube (Figure 9). It was observed that a relatively larger population of small bubblets was produced in the water-methanol-air system than during the water only experiments.

Due to the near-wall location of small bubblets, they traveled at a lower upward speed than the larger-size bubblets observed with water only experiments.

Three specific flow patterns were identified in small diameter pipes: a. bubble (bubbly), b. train-of- bubbles[14] and c. pseudo-slug (see fig. 9). "H" bubbles were not detected. The bubble and pseudo-slug patterns were mainly observed with the 12 mm tubings.

The bubble and the train-of-bubble patterns were the only flow patterns observed with 7.8 and 4 mm tubings regardless of gas velocity and column of liquid h.

Instabilities

Averaged injection pressure (over 20 minutes constant gas injection step) and momentary pressure values (maximum and minimum recorded over five minutes) were used to quantify the level of instabilities. For each gas flowrate and tube used, the flow instability was calculated as a ratio (percent) between the maximum-minimum interval of momentary recorded pressure and the average injection pressure value. The percentage ratio of the maximum variation of pressure over the average pressure value was used as the indicator of the magnitude of flow instabilities (fig.10).

Using the occurrence of instabilities in excess of 10-20% and net production as a gas-lifting criteria, three flow regimes were generally observed: a. instable stage with bubble dissipation (no net production), b. instable stage with liquid production, and c. stable stage with liquid production.

Figure 10 illustrates the level of instabilities associated with production characteristics (superficial liquid velocity versus superficial gas velocity) and suggests that the occurrence of large instabilities condition did not significantly affect the liquid production trend.

Numerical Modeling

A summary of the existing gas lift models and their limitations as far as their applications for small diameter gas lifting is presented.

A new model adapted to small-diameter tubing was developed to evaluate better the onset of production and critical production condition (CPC) for both laboratory and field conditions.

Existing Gaslift Models

The conventional slug flow pattern (figure1) is composed of three major sub-patterns: a. a TD rising bubble, b. a swarm of "Harmathy" ("H") [16] type bubbles and, c. a fall-back liquid film.

Slug flow pattern for void fraction estimation

By combining the "H" Bubble and "TD" bubble characteristics, and using the empirical approximation of average void fraction in the liquid slug[15], Hasan[6] developed a model to determine the average local void fraction, (eqs. 8 a and 8 b):

$$\alpha = \frac{L_T}{L_U}\alpha_{TD} + 0.1 \quad \text{for } U_G^S \geq 0.4\,\text{m/s} \tag{8-a}$$

$$\alpha = \frac{L_T}{L_U}\alpha_{TD} + 0.25\,U_G^S \quad \text{for } U_G^S < 0.4\,\text{m/s} \tag{8-b}$$

The term α_{TD} in equations 8-a and 8-b represents the void fraction in the TD bubble section of a slug unit. The definition of the α_{TD} is given by the equation 9.

$$\alpha_{TD} = \frac{U_G^S}{U_G} = \frac{U_G^S}{C_o U_m + U_{t(T-D)}} \tag{9}$$

Terminal velocities TD[9] and H[16] bubbles can be calculated by using equations 10 and 11, respectively.

$$U_{t(T-D)} = 0.35\sqrt{gD\left(\frac{\rho_L - \rho_G}{\rho_L}\right)} \tag{10}$$

$$U_{tH} = 1.53\left(\frac{\Delta\rho\sigma g}{\rho_L^2}\right)^{0.25} \tag{11}$$

Hasan's[6] model considers the slip between the phases, but ignores the effect of fall-back film (an effect considered negligible for conventional tubing slug/gaslift situations).

Ansari's[5] model considers the slip between the phases as well as the effect of fall-back film (independent to interfacial tension). Ansari's model[5] uses the downward falling liquid film velocity U_{LTB} as described by Brotz[17] :

$$U_{LTB} = \sqrt{196.7 g \delta_L} \tag{12}$$

where the film thickness δ_L is:

$$\delta_L = \frac{D}{2}(1 - \sqrt{\alpha_{TD}}) \quad (13)$$

Visual observations performed during this study indicated that "Harmathy" bubbles can not develop in small-diameter tubing. However, existing models[5-6] for conventional gas-lifting in large diameter (D>1 in) tubings were developed by considering the presence of Harmathy bubbles.

Both Ansari[5] and Hasan[6] models were used for comparison. Figure 11 compares the laboratory gaslift production data with the Ansari's model predictions. For 12 mm diameter tubing, and h=63.5 cm (S= 20%) and L=3 m. Hasan's model failed to indicate any net production, therefore, is not included in the figure 11.

It is observed in figure 11 that the Ansari's model of liquid production rates is underestimating laboratory measurements by about 60%.

Another observation is related to the critical gas flowrate at CPC (identified for the minimum gas injected where a net production of liquid was first observed). Ansari model predicts the onset of the liquid production at a superficial gas velocity of 0.75 m/s. However, the measured gas superficial velocity corresponding to the CPC was 0.4m/s. Ansari model, therefore, over predicts the gas injected at CPC by about 80%.

Comparison of the experimental data with the model predictions has clearly shown that there is a need for the development of a model capable to project laboratory results with small-diameter gas lift to a field scale, particularly for depth in excess of 100 m. Therefore, aiming at a better evaluation of critical production conditions an in-house model was developed.

The Critical Production Conditions (CPC) Model

The critical production conditions (CPC) model was developed to provide rapid estimation of critical field conditions and screening criteria for selection/elimination of various potential candidates for "small-diameter gas lift operations".

Equation 14 illustrates the pressure balance for any gaslift operation where the sum of the static and the frictional pressure drops (at a certain gas-liquid transport condition) is equal the reservoir pressure.

$$P_{Res} = \rho_l g h = \sum_{H=0}^{H} \left[\left(\frac{dP}{dL} \right)_{st} + \left(\frac{dP}{dL} \right)_{fr} \right] \quad (14)$$

The frictional and static pressure drops are estimated by using equations 15a and 15 b, respectively.

$$\left(\frac{dP}{dL} \right)_{fr} = f_M \frac{\rho_m U_m^2}{2D} (L + h) \quad (15\text{-a})$$

$$\left(\frac{dP}{dL} \right)_{st} = \rho_m g (L + h) \quad (15\text{-b})$$

Where the local two-phase density ρ_m is calculated by using the local void fraction α in the equation 16.

$$\rho_m = \bar{\alpha}\rho_G + (1 - \bar{\alpha})\rho_L \quad (16)$$

By combining the equations 15-a, 15-b and 16, the expression for the void fraction, which satisfies the pressure balance, (eqn.14) can be developed as shown in the equation 17.

$$\bar{\alpha} = \frac{\rho_l}{\rho_l - \rho_G} \left[1 - \frac{g h}{L \left(g + f_M \frac{U_m^2}{2.D} \right)} \right] \quad (17)$$

The liquid film thickness is given by the equation[14] (18):

$$\delta = 0.32 D (3 Ca)^{2/3} \quad (18)$$

where Ca is the capillary number:

$$Ca = \frac{\mu U_{film}}{\sigma} \quad (19)$$

Equations 18 and 19 are used to calculate the thickness of the downward flowing film as function of interfacial tension and viscosity. The effect of wavy film interface was not considered in the derivation of the model.

At the CPC point, a linear variation of the void fraction was assumed between the injection and production levels (i.e. along the well); this assumption represents the best CPC (critical production condition). The model was first used to assess the effect of tube length (well depth) for various tube diameter and reservoir pressure and determine (the required gas injected) at the CPC (the moment a net liquid production is recorded). The model was first validated using laboratory data.

Verification CPC Model

Laboratory data obtained from gas lifting experiments with 7.8 mm and 12 mm diameter tubes were used to validate the CPC model.

The first set of experiments used for CPC model validation was conducted in 7.8 mm diameter tube with a specific gas injection rate of 0.206 m/s. The three experimental data points shown in figure 12 were measured at h=38.1, 50.8 and 63.5 cm (corresponding to reservoir pressures of 4, 5, and 6.2 kPa respectively). The model predictions of critical depth (i.e. maximum possible depth the well can produce at a prescribed gas injection rate) agrees reasonably well with the laboratory-measured values.

The second group of experiments used for model validation were conducted by using the 12 mm diameter tube at specific gas injection rates of 0.316 m/s and 0.707 m/sec (fig. 13). The CPC model predictions of critical depth also agreed well with the experimental data in this case and results were further extrapolated to typical field depth.
For example; for a reservoir pressure of 3.7 Kpa and Usg=0.326 m/s, the model predicted critical depth as 2.1 m while the measured critical depth for this case was 1.81 m (14% difference). The maximum difference recorded between measured and calculated values of critical depth was less than 18%.
The CPC model was also used for prediction of field-scale critical depth using 12 mm diameter tubing for gas lifting. As shown in figure 13, for a reservoir pressure of 400 KPa (equivalent to water column height of 40 m) and a specific gas injection rate of 0.707 m/s, the model predicted critical depth as 300m. The calculated submergence for this example was 13%.
The model was further used to investigate field-simulated situations for a large range of tubing diameters. The critical depth is defined (for a certain D, reservoir pressure and gas injected rate) as the maximum depth at which a threshold production condition is achieved.
Figure 14 compares critical depth for a reservoir pressure of 400 kPa versus specific gas injection rates (expressed as superficial gas velocities) for D=7.8, 12 and 25 mm tubes.

For superficial gas velocities lower than 1.5 m/s and 400 kPa reservoir pressure, it appears that using a 7,8 mm tube will allow for an increased depth. However, if the superficial gas velocity increase beyond 1.7 m/s the situations may change, mainly because of the influence of increasing frictional pressure drop. Also, it should be noted that the advantage obtained from the use of 7,8 mm versus 12 mm tubing is not significant, for practical reasons, using a 12 mm tubing may be favored.

Future work

To improve the understanding on the effects of liquid film fallback and extend the model from limiting, threshold production estimations to calculations of actual production situations, additional laboratory work will be performed with both conventional and small-diameter tubes using liquid mixtures of various interfacial tensions

Conclusions

1. An experimental and numerical modeling study has been conducted to investigate advantages and limitations of using small-diameter tubes for extreme gas lifting conditions.

2. Replacing conventional large diameter tubings (D>1 in) with small-diameter tubings (D < 1 in) offers potential advantages for unloading water and resuming production from gas wells with low reservoir pressure.

3. An experimental apparatus was designed and operated to produce salient proof of the concept of gas lifting using small diameter tubings. Experimental data have been further used to develop a model for assessing critical conditions of the process in the field applications. Laboratory validation of the new (CPC) model indicates a range of errors under 18%.

4. The new model reflects the capillarity effect observed through the fall-back of liquid film better than conventional gas lift models. The liquid film fall-back is a key limiting factor for transfer of liquids within the few hundred meters. Maximum liquid transportation depth (i.e., critical depth) was numerically determined for various field-limiting conditions including low reservoir pressure and gas-liquid flowrates

5. Laboratory tests were able to identify and quantify the occurrence of flow instabilities reflected through significant oscillations of total (static and dynamic) transport pressure. It appears that instabilities do not negatively affect the average liquid production.

Acknowledgments

The authors would like to acknowledge the support and technical input of Mr. Ray Ivey. Dr Alex Turta for valuable discussions and suggestions regarding the physics of this problem of “small diameter tubes”. Mr. Sean Watt for contributions in designing and building of the experimental set up. IRAP – NRC-CNRC program and P R Toma Consulting Ltd. for the support given to this project during 2003-2004 and permission to publish.

Nomenclature

BHP	bottom hole pressure
Co	distribution coefficient, usually Co=1.2
CPC	Critical Point Condition
D	inside tube diameter (mm)
f_M	Moody friction factor
g	acceleration of gravity, (m/s^2)
h	length of liquid column (m)
L	length of tube (m)
L_T	L_{T-D} Taylor-Dumitrescu bubble length (m)
L_U	slug unit length (m)
P_{res}	reservoir Pressure (kPa)
ΔP_{st}	static pressure loss (Pa)
ΔP_{fr}	frictional pessure lss (Pa)
Q_G	gas flowrate (l/min)
Q_L	liquid flowrate, (l/min)
S	submergence (eq. 5)
TD	Taylor-Dumitrescu bubble.
H	Harmathy bubble.
U_G^S	superficial gas velocity, also U_{gs}, (m/s).
U_L^S	superficial liquid velocity, also U_{ls} (m/s).
U_G	gas velocity (m/s)
U_{LTB}	fall-back liquid film velocity (m/s)
U_t	Bubble terminal velocity (m/s)

Greek Symbols

α	αverage void fraction slug unit.
α_{TD}	void fraction at the Taylor-Dumitrescu bubble section.
α_{SU}	void fraction whole slug unit
δ_L	film thickness (m)
ρ_L	density of liquid phase (m^3/s)
ρ_G	density of Gas phase (m^3/s)
ρ_m	density of the mixture, (m^3/s)
σ	interfacial tension [N/m= (Dyne/cm)/1000]

References

1. Eicher H. V. Jr.: “The History of Gas Lift and Its Modern Application to the Petroleum Industry”. The Petroleum Engineering Journal, January 1952.

2. Brown, E.K.:”Overview of artificial lift systems,” JPT, Oct. 1982, pp2384-2396.

3. Govier, G.W. and Aziz,K., The flow of complex mixtures in pipes, Van Nostrand Reinhold, 1972.

4. Brill, J.P. and Mukherjee, H. Multiphase flow in wells, SPE Monograph Series, v. 17, 1999.

5. Ansari A. M., Silvestre N.D., Sarica C., Shoham O., Brill J.P.: “ A Comprehensive Mechanistic Model for Upward Two-Phase Flow in Wellbores”. SPE Production & Facilities. SPE 20630. pp. 143-151. May 1994.

6. Hasan A. R.: “Void Fraction in Bubbly and Slug Flow in Downward Vertical and Inclined Systems”, SPE Production and Facilities. SPE 26522.pp. 172-176. August 1995.

7. Nicklin D. J., Wilkes J. O., and Davidson J. F.: “ Two-Phase Flow in Verical Tubes”. Trans. Inst. Of Chem. Engrs. Vol. 40. pp. 61. 1962.

8. Toma, P., Landry, B., Schubert, L. and Miller, C.:”Field Results of Waterflood Enhancement Using a Gas Lifting Strategy,” paper CIM 96-32 (presented at 47th CIM Meeting, Calgary, June 1996).

9. Dumitrescu, D.T., “Stromung an einer Luftblase im senkrechten Rohr”, Z. angew. Math. Mech. 23, 3, Jun.1943, pp. 139-149.

10. Hinze, J.O., “ Fundamentals of the Hydrodynamic Mechanism of Splitting in Dispersion Processes”. AIChE J., Vol. 1, pp. 289. 1955.

11. Reinemann D. J., Parlange J. Y. and Timmmons M. B.: “ Theory of Small-Diameter Airlift Pumps”, Int. J. Multiphase Flow Vol. 16 No. 1, pp. 112-122, 1990.

12. De Cachard F., Delhaye J.M: “ A Slug-Churn Flow Model for Small-Diameter Air Lift Pumps”. Int. J. Multiphase Flow. Vol. 22. No. 4. pp. 627-649. 1996.

13. Bergles A.E., collier J. G., Delhaye J. M., Hewitt G.F., Mayonger F.: Two-Phase Flow and Heat Transfer in the Power and Process Industries”. Mac. Grew-Hill. Chapter 1. pp. 6-12. 1981.

14. Stark J., Manga M.: “The Motion of Long Bubbles in a Network of Tubes”. Transport in Porous Media. No. 40, 201-218. 2000.

15. Akagawa. K. and Sakaguchi T.: “ Fluctuation of Void Fraction in Two-Phase Flow “. Bull. JSME. V 9. pp. 104. 1966.

16. Harmathy, T.Z.: “Velocity of Large Drops and Bubbles in Media of Infinite or Restricted Extent.” AIChE J. Vol. 6, No. 2, pp. 281-288, June 1960.

17. Brotz, W.: ”Uber die Vorausberechnung der Absorptionsgesch-windingkeit con Gasen in Stromenden Flussigkeitsschichten,” Chem. Ing. Tech. No. 26, pp 470. 1954.

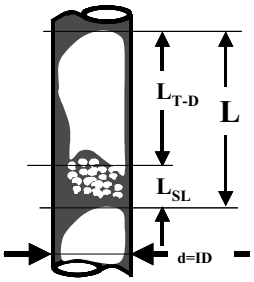

Figure 1 Schematic of slug flow features frequently observed with conventional gas lifting

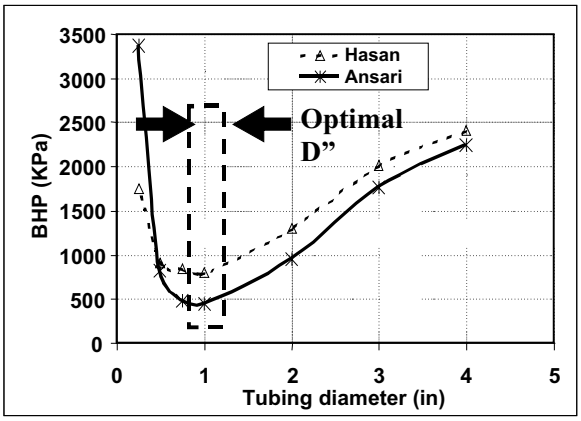

Figure 2 The effect of tubing diameter on the bottom hole pressure required for sustaining a fixed liquid production rate (numerical models) [H=200m, Q_L=1BBD (0.16 CMD), Q_G=15 MCFD]

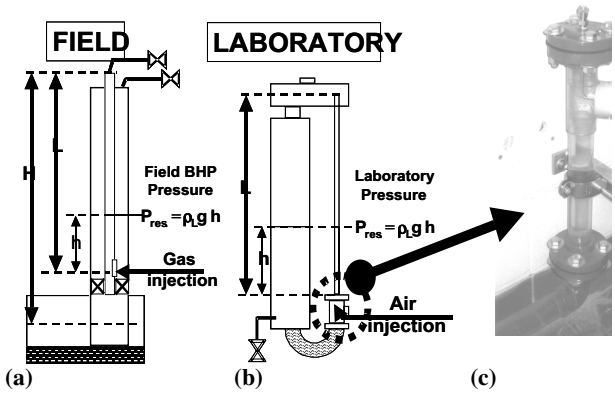

Figure 3 Schematic of field and laboratory gas lifting (a) Key elements of field gas-lifting . (b) Laboratory (c) gas injector device used in the laboratory (detail).

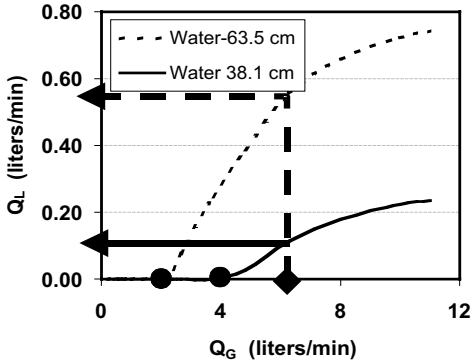

Figure 4 Influence of reservoir pressure on the liquid production rate (production characteristics for D=12mm and h= 63.5 and 38 cm - water only)

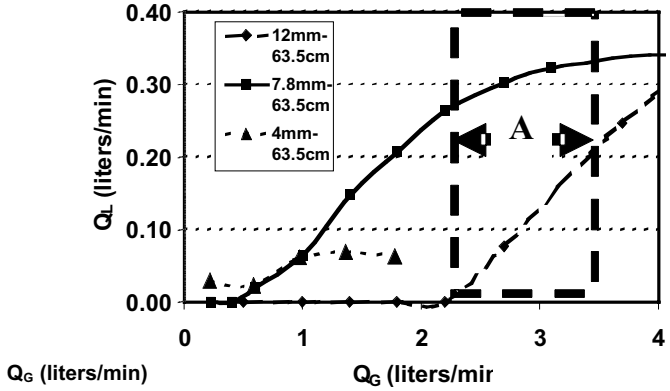

Figure 5 Liquid production versus gas injected for 12, 7.8 and 4 mm tubes at 63.5 cm fluid level (laboratory).

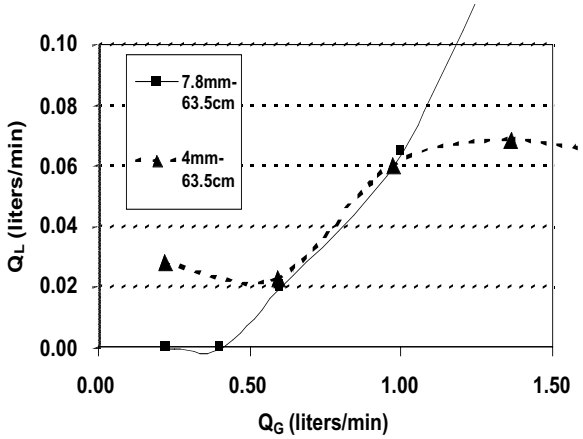

Figure 6 Liquid versus gas injected (D=4 mm, h=63.5 cm) detail - production characteristic at small laboratory gas injection

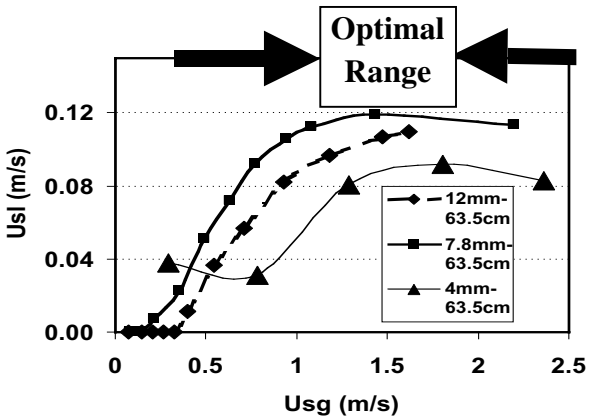

Figure 7 Production characteristics (superficial velocities) for D=4, 7.8 and 12 mm tubes at h=63.5 cm

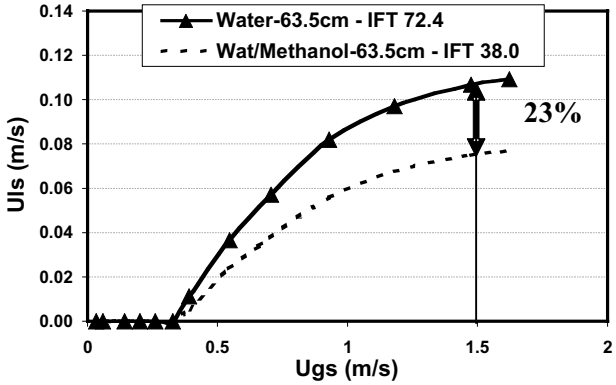

Figure 8 Superficial liquid velocity versus superficial gas velocity for water only and water-methanol (D=12mm, h=63.5 cm)

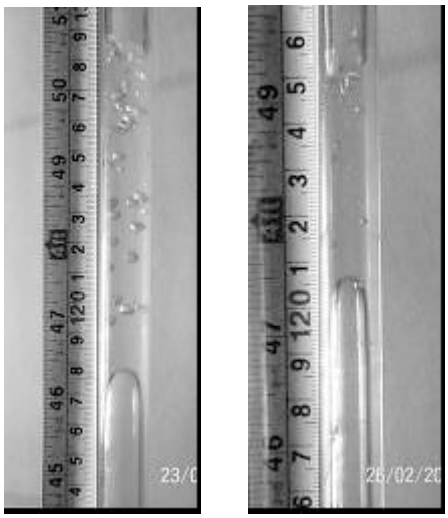

(a) (b)

Figure-9 (a) pseudo slug flow pattern with water only (D=12 mm, h=63.5 cm Ugs = 0.54 m/s Qg =3.7 l/ min) (b) train-of-bubbles with water-methanol (D=7.8 mm, h=63.5 cm, Ugs = 0.21 m/s, Qg = 0.6 l/min, σ= 38 dyne/cm)

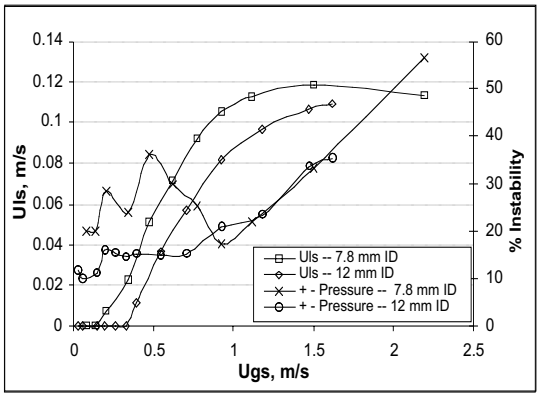

Figure 10 Flow instabilities with water flowing in a 12 mm and 7.8 mm ID tube

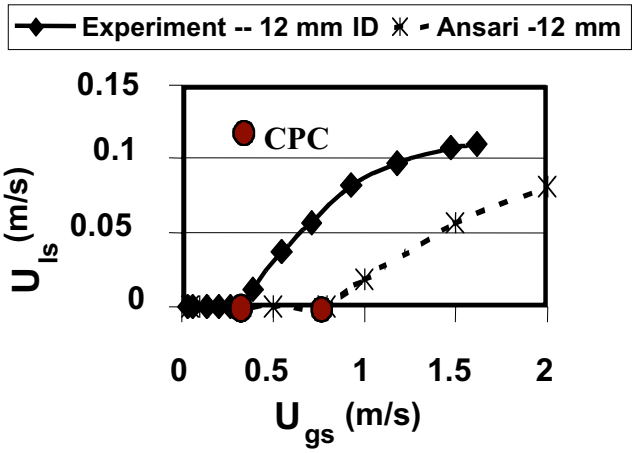

Figure 11 Comparison of laboratory data and model prediction of liquid production rate (D=12 mm, h=63.5 cm)

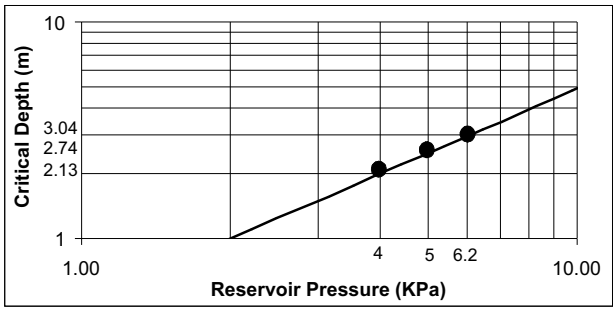

Figure 12 CPC model prediction of critical depth versus laboratory-measured values (D=7.8 mm Q_{gs}= 0.234 m/s)

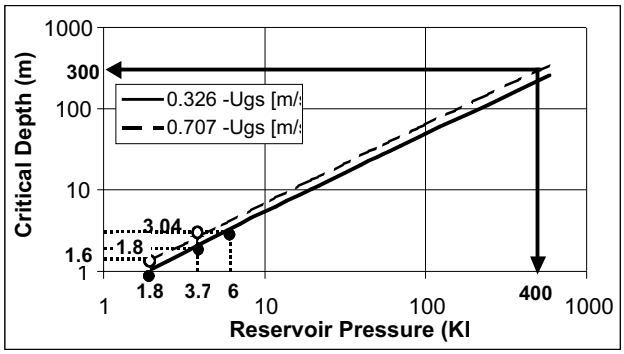

Figure 13 Critical depth versus reservoir pressure (CPC simulated field conditions for D=12 mm, U_{gs}=0.33 and 0.71 m/s)

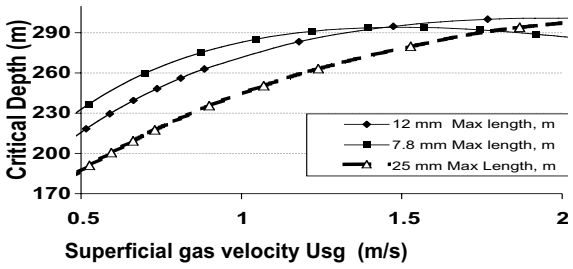

Figure 14 critical depths versus superficial gas velocity for 7.8, 12 and 25 mm tubing (reservoir pressure 400 KPa - 58 psi).